Investigation of the artificial saliva and saline droplet size measurement accuracy for COVID-19 infection control

Thomas Y. Wu [a,1], Yi-Hung Liu[b], Fang-hsin Lin[b] , Yue Liu[c], Junjie Liu[c], Jinsang Jung[d], Wesley Zongrong Yu[e,2], Qinde Liu[e], Richard Y.C. Shin[e], Tang Lin Teo[e]

[a] *National Metrology Centre (NMC), Agency for Science, Technology and Research (A*STAR), 8 CleanTech Loop, #01-20, Singapore 637145, Republic of Singapore*

[b] Center for Measurement Standards, Industrial Technology Research Institute (CMS/ITRI), Hsinchu 30011,Taiwan

[c] National Institute of Metrology (NIM), No.18, Bei-San-Huan Dong Str., Beijing 100029, China

[d] Korea Research Institute of Standards and Science (KRISS), 1 Doryong Dong, Yuseong Gu,Daejon , 305-340, Korea

[e] Chemical Metrology Laboratory, Chemical Metrology Division, Applied Sciences Group, Health Sciences Authority (HSA) of Singapore, 1 Science Park Road, #01-05/06, The Capricorn, Singapore Science Park II, Singapore 117528, Singapore

ABSTRACT

The size of human speech or cough droplets decides their air-borne transport distance, life span and virus infection risk. We have investigated the measurement accuracy of artificial saliva and saline droplet size for more effective COVID-19 infection control. A spray generator was used for polydisperse droplet generation and a special test chamber was designed for droplet measurement. Saline and artificial saliva were gravimetrically prepared and used to generate droplets. The droplet spray generator and test chamber were circulated as travelling standard among four metrology institutes (NMC, CMS/ITRI, NIM and KRISS) for droplet size measurement comparison and evaluation of deviations. The composition of artificial saliva was determined by measuring the mass fraction of the inorganic ions. The density of dried artificial saliva droplets was estimated using its composition and the density of each non-volatile component. The volume equivalent diameter (VED) of droplets have been measured by aerodynamic particle sizer (APS) and optical particle size spectrometer (OPSS). As a response to the COVID-19 pandemic, this is the first time that a comparative study among four metrology institutes has been conducted to evaluate the accuracy of saliva and saline droplet size measurement. For artificial saliva droplets measured by OPSS, the deviations from the reference VED (~4 μm) were below 5.3%. For saliva droplet sizes measured by APS, two institutes showed higher deviations up to 21.9% from the reference VED. For saline droplets measured by APS, the deviations from the reference VED were below 10.0%. The potential droplet size measurement errors using OPSS and APS have been discussed. This work underscores the need for new reference size standards to improve the accuracy and establish traceability in saliva and saline droplet size measurement.

Keywords*: aerosol metrology, droplet sizing, optical particle size spectrometer, aerodynamic particle sizer, saliva droplet, infection control*

1. Introduction

The spread of coronavirus disease (COVID-19) has been reported to be caused in part by the release of infectious droplets and aerosols when infected individuals cough, sneeze or speak

[1] Corresponding author: Thomas Y. Wu, email: yongusa@qq.com

[2] Present address: National Centre for Food Science, Singapore Food Agency (SFA), 7 International Business Park, Singapore 609919

(Wang et al. 2021; Asadi et al. 2020; Morawska and Cao 2020). It is important to study the droplet size distribution around a person after he/she coughs, sneezes or speaks. These infectious droplets will evaporate and shrink to become small-size aerosols, which can stay in the air for a longer period of time and travel a longer distance to cause more infections (Fennelly 2020; NASEM 2020; Gralton et al. 2011; Chao et al. 2009; Langmuir 1951; Duguid 1946; Wells 1934). It is important to know the final size of such droplets after evaporation, which will decide their air-borne transport distance, life span and risk of virus infection (De Oliveira et al. 2021; Randall et al. 2021; Rezaei and Netz 2021; Chaudhuri et al. 2020; NASEM 2020; Netz 2020; Netz and Eaton 2020; Bourouiba 2020; Bourouiba et al. 2014; Redrow et al. 2011; Xie et al. 2007; Nicas et al. 2005). These information are needed for risk assessment in the context of recommending and implementing appropriate risk management measures such as safe distancing, segregation, risk mitigation in public area and hospital environment.

There have been a lot of research work on human breath, speech, cough and sneeze droplets size measurement. High variability in measured size distribution of such droplets have been found in literature (Bourouiba 2020, 2021; Stadnytskyi et al. 2020; Morawska et al. 2009; Papineni and Rosenthal 1997). The expired droplets from sneezes or coughs have a counting peak in 2-4 μm in size distribution (with falling height of 5 ft) (Duguid 1946). Optical particle counter (OPC) was used to measure human breath droplets, which shows a counting peak at 0.6 to 1 μm in diameter size distribution (Papineni and Rosenthal 1997). The human speech and cough droplets were measured by interferometric Mie imaging technique to show a peak at 4-8 μm in size distribution at 60 mm distance (Chao et al. 2009). Human cough droplets were measured by an aerodynamic particle sizer (APS) and their size distribution had shown a peak at 0.7 – 2.1 μm (Yang et al. 2007). Measurements using APS have shown that speech droplets have multimodal size distribution with peaks around 0.5-0.8, 1.8, 3.5 and 5 μm (Morawska et al. 2009). Laser light scattering and movie recording were used to estimate the human speech droplets' size to be around 4 μm (after full evaporation) based on the weighted average decay rate of droplets (Stadnytskyi et al. 2020).

Various measurement techniques are not harmonised and there is a lack of reference standards in such droplet size measurement. To the best of our knowledge, a detailed evaluation of the measurement accuracy in saliva droplet size has not been reported in literature. Metrology reference standards and measurement methodology guide are needed in this critical area to ensure more accurate droplet size measurement for reliable infection control. As part of Asia Pacific Metrology Programme (APMP)'s response to the ongoing COVID-19 and future pandemics, a research project has been carried out to study the saliva droplet size measurement methodology and measurement accuracy (Wu 2022). This is the first time that artificial saliva and saline droplet size measurements (~ 4 μm) have been evaluated via a travelling standard which was circulated among several metrology institutes: National Metrology Centre (NMC) of

A*STAR, Center for Measurement Standards of the Industrial Technology Research Institute (CMS/ITRI), National Institute of Metrology of China (NIM) and Korea Research Institute of Standards and Science (KRISS). APS and optical particle size spectrometer (OPSS) are used in this comparative study to measure the droplets generated by the travelling standard. This paper will describe the experiment designed to generate saline and artificial saliva polydisperse droplets, a specially designed test chamber, test liquid preparation, composition analysis for artificial saliva, droplet size measurements by four metrology institutes. We will present our analysis of the droplet measurement results and discuss the potential errors and traceability issues in droplet size measurement.

2. Droplet measurement setup and methodology

2.1 Droplet generator and test chamber

A portable ultra low volume (ULV) sprayer was selected as droplet generator (Longray, model: 2680A) to produce saline or artificial saliva droplets. High-pressure air and liquid are introduced to a two-fluid nozzle to produce polydisperse droplets (Kramm et al. 2023; Nasr et al. 2002; Nguyen and Rhodes 1998). The turbulent air induce dynamic pressure forces which overcome the surface tension forces and break the liquid into fine droplets. The liquid flowrate can be adjusted, with higher flowrate leading to larger droplets. The ULV sprayer has shown good repeatability in droplet volume-size distribution. Each lab use the same knob setting for liquid flowrate control of the sprayer, with liquid flowrate at ~40 mL/min. 3 types of droplet were generated by the ULV sprayer: saline 18.1% (w/w), saline 6.5% (w/w) and artificial saliva. The preparation of saline and composition analysis of the artificial saliva will be given in section 3.

We have designed and developed a droplet test chamber for droplet size measurement. The chamber is a tube with length of ~1 m and diameter of ~0.6 m, as shown in Fig 1. It is equipped with a blower fan and HEPA filter at the air inlet and outlet. The aerosol particle concentration background level is reduced to below 3 cm^{-3} inside the chamber via the clean air being blown into the chamber for flushing.

When the air flushing is completed, saline or artificial saliva droplets are sprayed into the chamber for measurement by the droplet sizer, as shown in Fig 2. There are two sampling locations used for our measurement experiment: port 1 and port 3, which is about 40 cm and 75 cm from the spray nozzle respectively.

Fig. 1. A CAD drawing for the droplet test chamber. The droplet generator is connected to the left side of the chamber for ejection of droplets into the chamber. Clean air is blown from left side to flush the chamber before each measurement experiment.

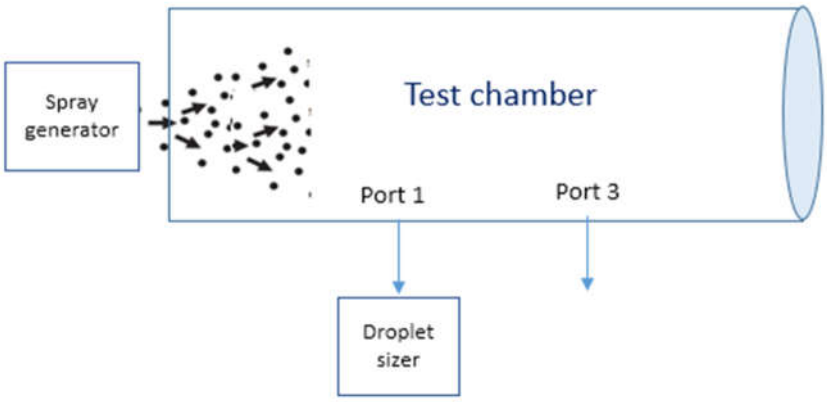

Fig. 2. A test setup diagram to show the droplet spray generator, test chamber, sampling ports and droplet sizer (sampling is done at port 1 or port 3).

The droplets are ejected into the chamber for measurement after the minimum particle concentration background level is obtained. Droplet size measurement is started when the droplet number concentration inside the chamber is stabilized. After each round of droplet spraying and measurement, the chamber is flushed again by clean air to remove the residual droplets.

The ULV spray generator and the test chamber are used as the travelling standard, which was circulated among four metrology institutes (CMS/ITRI, KRISS, NIM and NMC) for measurement of saline and artificial saliva droplet size. The same batch of test liquids were also provided to each laboratory for the measurement experiment. Each laboratory used their own commercial particle sizer to measure the saline and artificial saliva droplets.

2.2 Droplet size measurement

Droplets were sampled at port 1 and port 3 separately. Port 1 and port 3 is about 40 cm and 75 cm from the spray nozzle, respectively. Droplets were measured by two types of commercial particle sizer: OPSS (Grimm 11-D) used by NMC, and APS (TSI 3321) used by CMS/ITRI, NIM and KRISS .

In a single-particle OPSS, the scattered light is collected and analysed to determine the particle size based on the refractive index and scattering angle (Czitrovszky 2010; Szymanski et al. 2009; Bemer et al. 1990; Szymanski and Liu 1986; Liu et al. 1985; Chen et al. 1984; Mäkynen et al. 1982; van der Meulen et al. 1980). When particles flow through a measurement cell, wide-angle light scattering signals are collected by the detector inside the Grimm 11-D. An OPSS need to be calibrated by metrology standards to ensure high accuracy in aerosol particle size and number concentration measurement (Wu et al. 2022a, 2022b; Vasilatou et al. 2020, 2021; Sang-Nourpour and Olfert 2019; Iida and Sakurai 2018; ISO 2009, 2018; Iida et al. 2014; Yli-Ojanperä et al. 2012). The Grimm 11-D classifies particles into 31 logarithmic-scale equidistant channels with high size resolution. The particle size range of Grimm 11-D is from 0.25 to 35 μm. The sampling flowrate of 11-D is 1.2 L/min with a sampling interval of 6 seconds.

An APS accelerates the aerosol particle samples through an internal accelerating orifice. The aerodynamic size of the particle is derived via its measured rate of acceleration, since larger particles have a slower acceleration due to its larger inertia. After exiting the nozzle, the particles cross through two laser beams which are partially overlapped in the detection area. The configuration of the detection area has been designed to improve the particle detection efficiency and reduce the Mie-scattering oscillations in measuring the light-scattering intensity. Lots of research work have been conducted to study the particle sizing accuracy of APS (Chien et al. 2016; Baron et al. 2008; Peters et al. 2006; Heidenreich et al. 1995; Marshall et al. 1991; Ananth and Wilson 1988; Wang and John 1987; Baron 1986; Chen et al. 1985; Griffiths et al. 1984) . The particle size measurement range of TSI 3321 is 0.5 to 20 μm (in 52 size channels), with a total particle sampling flowrate of 5 L/min and sampling interval of 5 seconds.

It has been shown that, for human speech droplets, the evaporation to the equilibrium droplet size occurs within 0.8 second (De Oliveira et al. 2021; Redrow et al. 2011; Morawska et al. 2009). Thus we have assumed the measured droplets in the measurement cell by the particle sizer in our case are fully dried, considering the sampling time of sizing instrument and the transit time from sprayer nozzle to the measurement cell.

2.3 Definition of measurand for comparison

To ensure all four metrology institutes measure the same parameter in this comparative study, we have defined the volume equivalent diameter (VED) of each size channel *i* (of particle sizer) as:

$$d_{\mathrm{i}} = \left[\frac{d_{2,i}^4 - d_{1,i}^4}{4(d_{2,i} - d_{1,i})}\right]^{1/3} \qquad (1)$$

where ($d_{1,i}$, $d_{2,i}$) is the lower and upper bound for size channel *i*. The total volume concentration (TVC) for droplets detected in channel i is estimated as:

$$\mathrm{V_i} = \mathrm{C_i}\,(\pi d_i^3)/6 \qquad (2)$$

where $\mathrm{C_i}$ is the measured number concentration of channel i.

There is a peak in the TVC-size distributions as measured by particle sizer for saline and artificial saliva droplets. We have defined the measurand (Mari 2015; Pavese 2007) of this comparison to be the VED size corresponding to the channel with a peak in the droplets' TVC-size distribution. The VED (d_{i}) for the channel with maximum $\mathrm{V_i}$ is measured for multiple times. Their mean value for each liquid type and sampling port is reported by each metrology institute for comparison and evaluation of droplet size measurement.

For measurement by OPSS, the optical diameters of each size channel reported by Grimm 11-D were used to derive the VED (d_{i}) directly. For measurement by APS, the aerodynamic size (d_a) from TSI 3321 need to be first converted to optical equivalent diameter d_o which is given by

$$d_o = \sqrt{\frac{X}{\rho_p}}\, d_a \qquad (3)$$

where ρ_p is the droplet's material density, χ is the droplet's dynamic shape factor (DSF) (Kuwata and Kondo 2009; Wang et al. 2009; DeCarlo et al. 2004) .

3. Test liquid for droplet generation

Various type of liquids have been used for droplet generation and evaporation study in published literature [13-18]. We decided to use 6.5% and 18.1% (w/w) saline solutions and artificial saliva (with mucin, stabilized) to generate droplets. The artificial saliva droplets are used to simulate the human speech or cough droplets. The saline droplets are used for cross-checking droplet size measurement accuracy, since they have different material density, shape and evaporation process.

3.1 Saline solution preparation

Sodium chloride (NaCl) standard reference material (SRM 919b) were purchased from National Institute of Standards and Technology (NIST, Gaithesburg, MD, USA). The saline solutions were prepared using gravimetric method by dissolving SRM 919b with Type 1 ultrapure water (having a resistivity >18 MΩ-cm at 25°C). The purity of NIST SRM 919b is 99.835% ± 0.020%. The

certified mass fraction Chloride ions and Sodium ions (in SRM 919b) is 60.564% ±0.014% and 39.2747% ±0.0075%, respectively.

A precision balance (Sartorius, Model: Entris 6202I-1S) with readability of 0.01 g was used to weighthe ultrapure water, and a top loading balance (Sartorius, Model: MSA323S-100-DE) with readability of 0.001 g was used to weighi the NaCl. The NaCl was dried for 3 h at 110 °C in an oven, then stored in a desiccator over anhydrous magnesium perchlorate for about 1 h. The 6.5% and 18.1% (w/w) saline solution were prepared by weighing a pre-calculated amount of dried NaCl in a dish then carefully transferred into a pre-cleaned 2L glass bottle. A pre-calculated amount of ultrapure water was added into the glass bottle and the total weight was recorded.

3.2 Artificial saliva composition analysis

The artificial saliva (with mucin, stabilized) materials were produced by Pickering Laboratories (Product No.: 1700-0316) and were used in our study to produce the saliva droplets. It should be noted that Pickering Laboratories prepared the materials according to ASTM E2720-16 and ASTM E2721-16 (ASTM 2016b, 2016a). The preparation mass of the components in the artificial saliva are shown in Table 2. We have determined the mass fraction of each component based on the measured concentration of inorganic ions in the artificial saliva.

The mass fraction values of total magnesium (Mg), calcium (Ca), sodium (Na), potassium (K) and chloride (Cl) in the artificial saliva sample were determined using exact-matching isotope dilution mass spectrometry (IDMS) method measured by either inductively coupled plasma-mass spectrometry (ICP-MS) or inductively coupled plasma high resolution-mass spectrometry (ICP-HR-MS) (Yu et al. 2021; Xu et al. 2017; Liu, H.; Xu, B.; Cao, W-L.; Dai 2010; Sargent et al. 2002). Standard reference materials (SRM) from the NIST: Mg (SRM 3131a), Ca (SRM 3109a), K (SRM 918c) and Cl (SRM 919b), were used as the calibration standards. Enriched isotopes ^{25}Mg, ^{42}Ca, ^{41}K, and ^{37}Cl from the Oak Ridge National Laboratory (USA) were used as the internal standards. We have prepared the calibration blends gravimetrically by mixing appropriate amounts of calibration standard solution and internal standard solution. The sample blends were prepared by spiking appropriate amounts of internal standard into the sample before dilution. Depending on the analyte, 0.10 – 1.00 g of sample was diluted with appropriate amount of HNO_3 and allowed to equilibrate at room temperature for more than 12 h.

For the determination of Mg, Ca and K, the diluted blend mixtures were centrifuged and the supernatant was collected and further diluted to achieve the desired concentration for optimum measurement by ICP-MS (for Mg) or ICP-HR-MS (for Ca and K). For the determination of Cl, the method involved the separation of protein by precipitation and centrifugation, followed by the precipitation of Cl by adding appropriate amount of silver nitrate solution. The silver chloride precipitate was washed with Type 1 water and re-dissolved in appropriate amount of ammonium solution before analysis by ICP-HR-MS (Yu et al. 2021).

The mass fraction value of sodium in the artificial saliva sample was determined by internal standard (ISTD) addition method using ICP-MS. Na (SRM 919b) and Al (SRM 3101a) SRMs from NIST were used as the calibration standards and the internal standards, respectively. The calibration blends were prepared gravimetrically by mixing appropriate amounts of calibration standard solution and internal standard solution. We have prepared the sample blends by spiking appropriate amounts of internal standard into the sample before dilution. 0.5 g of sample was diluted with appropriate amount of HNO_3 and allowed to equilibrate at room temperature for more than 4 h. The diluted blend mixtures were centrifuged, and the supernatant was collected and further diluted to achieve the desired concentration for optimum measurement by ICP-MS.

The mass fraction value of urea in the artificial saliva was determined by liquid chromatography-isotope dilution tandem mass spectrometry (LC-IDMS/MS) method. The urea (SRM 912b) SRM from NIST was used as the calibration standard. The enriched isotopes ^{13}C , $^{15}N_2$-urea were used as the internal standard. We have prepared the sample blends by spiking appropriate amounts of internal standard into the sample. The sample blends and calibration blends were then allowed to equilibrate at room temperature for 1 h.

We have diluted 0.10 g of artificial saliva sample with appropriate amount of acetonitrile and allowed it to equilibrate at room temperature for 10 min. The diluted blend mixtures were centrifuged, and the supernatant was collected and filtered before the analysis by LC-MS/MS.

Quality control material were also prepared and analysed concurrently with the analytes. Human sera certified reference materials (CRMs) from the Health Sciences Authority (HSA) comprising HRM-2005A (for total Mg, Ca, Na, K, and Cl) and HRM-3002B (for urea) were used. Frozen human plasma reference material from NIST, SRM 1950 (for total protein) was also used.

The measured mass fraction values (Table 1) of the analytes in the artificial saliva are traceable to the International System of Units (SI) through the use of calibration standards from NIST. The expanded uncertainty for the assigned value is listed, with coverage factor value *k* (approximately 95% confidence), estimated by combining uncertainties from the method precision, different ion pairs (for Mg and Ca only) used, isotope ratios, purity of the calibrant and weighing, according to ISO/IEC Guide 98-3:2008 Uncertainty of Measurement—Part 3: Guide to the Expression of Uncertainty in Measurement (ISO 2008).

Table 1 Measured mass fraction values of inorganic ions in the artificial saliva sample and their expanded measurement uncertainties.

Analytes	Mass fraction (mg/kg)		
	Assigned value	Expanded measurement uncertainty	Coverage factor, *k*
Mg	20.463	0.082	2.0
Ca	42.74	0.43	2.6
K	860	35	4.3
Cl	1191	25	4.3
Na	456.5	1.2	2.3
$(NH_2)_2CO$	124.8	1.6	2.0

The mass fractions of inorganic ions from the compounds used to prepare the artificial saliva was calculated, for comparison with the measured mass fractions of inorganic ions (Table 2). This comparison showed large deviation between the measured value and the calculated value for Mg, but small deviations for the rest inorganic ions.

Table 2 Comparison of measured mass fraction and calculated mass fraction of the inorganic ions in the artificial saliva.

			Mg	**Ca**	**Na**	**K**	**Cl**
Compounds in the artificial saliva (ASTM 2016a)	**Preparation Mass (g)**	**Molecular Weight (g/mol)**	**Calculated mass (g)**				
$MgCl_2.7H_2O$	0.04	221.30	0.00439	-	-	-	0.01281
$CaCl_2.H_2O$	0.13	128.98	-	0.04039	-	-	0.07145
$NaHCO_3$	0.42	84.00	-	-	0.11494	-	-
KH_2PO_4	0.21*	136.08	-	-	-	0.06021	-
K_2HPO_4	0.43*	174.17	-	-	-	0.09618	-
NH_4Cl	0.11	53.48	-	-	-	-	0.07290
KSCN	0.19	97.17	-	-	-	0.07645	-
$(NH_2)_2CO$	0.12	60.05	-	-	-	-	-
NaCl	0.88	58.44	-	-	0.34621	-	0.53379
KCl	1.04	74.54	-	-	-	0.54548	0.49452
Mucin Powder	3.00	-	-	-	-	-	-
Water	1019.36#	-	-	-	-	-	-
Total weight (g)	1025.93						
Inorganic ion			**Mg**	**Ca**	**Na**	**K**	**Cl**
Calculated mass fraction, X_i (mg/kg)			4.282	39.37	449.5	759	1156
Measured mass fraction, Y_i (mg/kg)			20.463	42.74	456.5	860	1191
Relative deviation, $(Y_i - X_i)/ Y_i$			79.1%	7.9%	1.5%	11.7%	2.9%

*The mass (g) were calculated by multiplying the reported volume (by converting mL to dm^3) with 0.2 M and their respective molecular weight (g/mol).
#The density of water was assumed to be 1 g/cm^3.

Based on the measured mass fraction of inorganic ions in artificial saliva, proportional correction of the preparation mass for the components (except for mucin) was made to match the measured total ion concentrations. With this approach, the mass fraction of non-volatile components in artificial saliva has been estimated. Our measurement showed an unexpectedly high concentration of Mg in the artificial saliva materials. After further investigation, we discovered that the addition of a preservative (containing MgO, with its mass fraction being estimated) during the production of the artificial saliva material accounted for the higher concentration of Mg measured experimentally. The mass fraction of mucin cannot be measured accurately due to high impurity in the mucin powder. Thus, the preparation mass of mucin (3.000 g, based on ASTM E2720−16) was used in estimating the mass fraction of non-volatile components. The composition of the fully dried artificial saliva was calculated (Table 3). The

preparation mass of component in artificial saliva sample is based on ASTM E2720−16. The mass fraction of the total non-volatile components in the artificial saliva is ~0.65%.

Table 3 Estimated composition of the fully dried artificial saliva (with mucin, stabilized (ASTM 2016a)) based on our measurement of the inorganic ions concentration in the artificial saliva.

Non-volatile components inside the artificial saliva	**Preparation mass** (ASTM 2016a), **g**	**Estimated mass based on ions' mass fraction measurement (except for mucin powder), g**	**Mass fraction**
$MgCl_2.7H_2O$	0.040	0.056	0.8%
$CaCl_2.H_2O$	0.130	0.141	2.1%
$NaHCO_3$	0.420	0.426	6.4%
KH_2PO_4	0.210	0.211	3.2%
K_2HPO_4	0.429	0.432	6.5%
NH_4Cl	0.110	0.131	2.0%
KSCN	0.190	0.192	2.9%
$(NH_2)_2CO$	0.120	0.126	1.9%
NaCl	0.880	0.893	13.4%
KCl	1.040	1.049	15.7%
Mucin powder	3.000	3.000	45.0%
MgO	-	0.018	0.3%

3.3 Material density of dried artificial saliva

The artificial saliva contains mucin powder (Sigma, mucin from porcine stomach, type II). The bulk density of the mucin powder was measured to be 0.681 g/cm^3 using the method A of WHO procedure (WHO 2020). The ratio of tapped density of porcine mucin powder to its bulk density had been measured to be 1.1615 (Eraga et al. 2016). Thus the tapped density of porcine mucin powder is derived as 1.1615 × 0.681 = 0.7913 g/cm^3 , which is used as the material density of mucin in the dried artificial saliva.

The composition of the dried artificial saliva is used to estimate its mean material density, which is calculated as the volume-weighted average using following formula (Hasan and Dzubay 1983) ,

$$\rho_{saliva} = \frac{1}{\sum_i \frac{MF_i}{\rho_i}} \qquad (4)$$

where ρ_i is the density of each chemical component and MF_i is the mass fraction for each component. Based on the estimated composition of dried artificial saliva, mass fraction for each component has be derived (Table 4). The density for NaCl is taken as 2.163 g/cm^3 , based on measurement given in (Johnston and Hutchison 1942). The density of mucin powder has been estimated to be 0.7913 g/cm^3 , and the densities of the rest non-volatile components in Table 4 are based on the values given in (Haynes 2016).

The material density of the fully dried artificial saliva droplet (after evaporation to equilibrium droplet size) is estimated to be 1.196 g/cm^3 using the composition and density of the non-volatile components as shown in Table 4.

Table 4 Estimation of the material density of dried artificial saliva droplet using its composition and the densities of the non-volatile components.

Component in dried artificial saliva	**Mass fraction**	**Density, g/cm³**
$MgCl_2.7H_2O$	0.8%	1.499
$CaCl_2.H_2O$	2.1%	2.240
$NaHCO_3$	6.4%	2.200
KH_2PO_4	3.2%	2.340
K_2HPO_4	6.5%	2.440
NH_4Cl	2.0%	1.530
KSCN	2.9%	1.890
$(NH_2)_2CO$	1.9%	1.320
NaCl	13.4%	2.163
KCl	15.7%	1.980
Mucin powder	44.9%	0.7913
MgO	0.3%	3.580
Mean density of dried artificial saliva, g/cm³		1.196

4. Droplet size measurement result

The effloresced artificial saliva droplets were shown to have an almost spherical shape in an SEM image (Walker et al. 2021) . It has been observed that evaporation of model saliva droplets (NaCl-mucin mixture or NaCl-protein mixture) will lead to amorphous phase surface shell of organic content and internal crystalline phase of NaCl which is enclosed by the semi-solid organic shell (Huynh et al. 2022). Thus, we can assume the shape of evaporated saliva droplet in our case is very close to a sphere, which would give lower light scattering compared to the cubic NaCl particles of similar size. We have used a DSF χ=1.0 for saliva droplets to calculate the VED for those reported saliva droplet sizes measured by APS of three laboratories.

The DSF for NaCl droplets has been estimated to be 1.17 for the VED size around 4 μm based on the study in (Zelenyuk et al. 2006) . The material density for dried saline droplet (NaCl) was taken as 2.163 g/cm³ based on measurement given in (Johnston and Hutchison 1942). From the estimated composition of artificial saliva (in section 3), the material density of dried artificial saliva droplet was estimated as 1.196 g/cm³. These values of DSF and material density have been used by CMS/ITRI, NIM and KRISS to convert their measured aerodynamic size of droplets to the optical equivalent diameter using (3) in order to obtain the VED for the peak position in the TVC-size distribution.

As an example, the TVC-size distributions measured by an APS for saline and artificial saliva polydisperse droplets are shown in Fig 3. There was a peak volume concentration at VED around 4 μm. The VED (d_i) for the channel with maximum V_i was reported by each metrology institute for comparison.

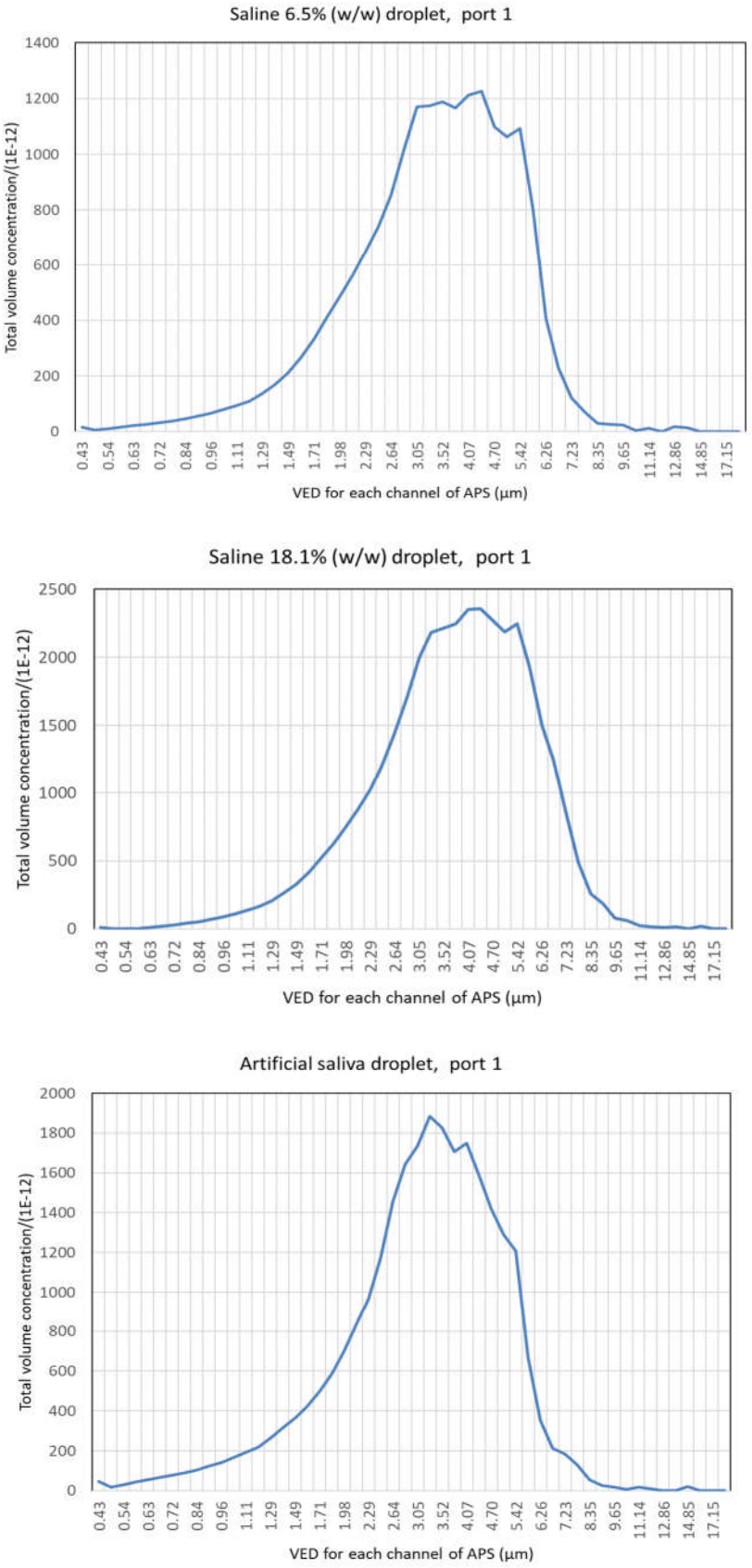

Fig. 3. The TVC-size distribution for 6.5% (w/w) saline, 18.1% (w/w) saline and artificial saliva polydisperse droplets measured by an APS at port 1 of test chamber. The measured aerodynamic diameters by APS were converted using (3) to derive the VED for each channel.

For each test liquid type and sampling port, the reported VED (d_i) from four institutes were averaged to obtain the mean value which served as the reference VED value (d_R):

$$d_R = \frac{\sum_i d_i}{4} \qquad (5)$$

The relative deviation of each institute's reported VED value from the reference VED value is then obtained as

$$D_i = \frac{d_i - d_R}{d_R} \qquad (6)$$

which is shown in Table 5.

Polystyrene latex (PSL) particles with certified diameter (near 4 μm) are used as traceable reference size standard to calibrate APS. The effective density of saline droplet can be estimated as $\rho_{saline}/\chi_{saline}$ =2.163/1.17 =1.849 g/cm^3 (Wu et al. 2022a; DeCarlo et al. 2004; Hand and Kreidenweis 2002). The effective density of saliva droplet can be estimated as $\rho_{saliva}/\chi_{saliva}$ = 1.196/1.0 = 1.196 g/cm^3.

The effective density of saline droplet is different from that of PSL particle which is about 1.05 g/cm^3. Based on previous studies (Ananth and Wilson 1988; Wang and John 1987; Baron 1986), the deviation of effective density of saline droplet from that of PSL particle could cause 6.4% oversizing error in saline droplet's aerodynamic diameter measurement using an APS (near 5 μm). Based on this theoretical correction factor, the oversizing errors have been corrected for saline droplet measurements using an APS.

The deviation of the effective density of saliva droplet from that of PSL particle could cause 1.4% oversizing error in saliva droplet's aerodynamic diameter measurement using an APS (near 5 μm). We have corrected the oversizing errors for saliva droplet size measurements using an APS via this theoretical correction factor, which had been derived in (Ananth and Wilson 1988).

Table 5 Relative deviation of four institutes' reported VED value from the reference VED for each test liquid type and sampling port. The assumed DSF is 1.17 for saline droplets and 1.0 for saliva droplets (with density correction factor applied for those measured by APS).

Sampling port	**Test liquid**	**Reference VED, μm**	**D_i (Relative deviation from reference VED)**			
			KRISS	**CMS/ITRI**	**NIM**	**NMC**
Type of measurement instrument			APS	APS	APS	OPSS
Port 1	Saline, 18.1% (w/w)	4.14	-1.6%	-6.5%	1.0%	7.1%
	Saline, 6.5% (w/w)	3.87	-9.7%	-8.7%	3.6%	14.8%
	Artificial saliva	3.93	20.8%	-21.9%	3.3%	-2.2%
Port 3	Saline, 18.1% (w/w)	4.31	2.4%	-10.0%	2.8%	4.9%
	Saline, 6.5% (w/w)	4.01	-8.8%	-3.3%	4.6%	7.5%
	Artificial saliva	3.94	17.8%	-20.2%	7.6%	-5.3%

For saline droplets, the measurement deviations (|Di|) of all institutes from the reference VED were below 14.8%. The measurement results of NIM and NMC showed smaller VED deviations for artificial saliva droplets, with |Di| ≤ 7.6%. Larger deviations in measured artificial saliva droplets' VED were found for those measured by APS at KRISS and CMS/ITRI. We can also see that, for measurements made by KRISS and CMS/ITRI, the VED deviation (D_i) of saline droplets is below 10.0%, much smaller than that of artificial saliva droplets.

From Table 5, the measured saline droplet size using OPSS exceeds the reference VED by 4.9% to 14.8%, which should be due to the increased light scattering from NaCl particles with non-spherical shape. It was shown that non-spherical NaCl particles (cubic shape) generate higher light-scattering compared to that predicted by Mie scattering theory for particles with spherical shape when particle diameter is beyond 0.8 μm (Chamaillard et al. 2003). Thus an OPSS would give oversizing error in measuring particles with irregular shape (Wu et al. 2022a; Gebhart 1991). The APS sizing measurement principle is not based on light-scattering, thus it is not affected by the NaCl particles' irregular shape.

The measured artificial saliva droplet sizes using OPSS show undersizing reading: smaller than the reference VED values by 2.2% and 5.3% for port 1 and 3, respectively. This is an indication that the light-scattering from saliva droplets are much lower compared to the cubic NaCl particles of similar size, since the shape of the artificial saliva droplet is close to a spherical shape. The deviation for the saliva droplet measurement by OPSS could be due to some variation in light scattering, since the refractive index of saliva droplet would be different from that of PSL particles used in OPSS calibration (McMeekin et al. 1962, 1964).

The deviations of NIM's measurement for saliva droplets using APS at both port 1 and port 3 are below 7.6%. But higher deviation of saliva droplets' VED (measured by APS) at KRISS and CMS/ITRI were observed, with overreading of 20.8% and underreading of 21.9%. It has been shown that, for liquid droplet with viscosity ≥ 0.1 Pa s, both oversizing or undersizing error are possible for droplet size near 4 μm (Bartley et al. 2000). The viscosity of human saliva has been measured to be 0.12 to 0.17 Pa s (Azodo and Osahon 2020). This high-viscosity of saliva droplet might be causing the higher deviation in the saliva droplet VED measured by APS: deviations of 17.8% & 20.8% in KRISS measurement and deviations of -20.2% & -21.9% in CMS/ITRI measurement, as shown in Table 5. However, the deviations for saline droplets measured by APS at these two laboratories are much lower (not affected by high-viscosity issues). The possible reasons for the higher deviations observed for saliva droplet measurement by APS will be discussed in section 5.

5. Discussion

The potential sources of measurement errors leading to the deviations in saline and artificial saliva droplet VED measurement are discussed in this section. The influencing factors include the spray generator effect, droplet density effect in APS measurement, refractive index deviations, droplet distortion in APS nozzles, conversion error from aerodynamic diameter to optical diameter (due to uncertainty in droplet's density and DSF), OPSS sizing error due to light-scattering variation, lack of reference standards for droplet size, etc.

5.1 Droplet distortion effect

There is potential undersizing error in APS due to the droplet distortion and focusing nozzle loading (with accumulated liquid) when it passes through internal orifice nozzle (Baron et al. 2008; Baron 1986). If the droplets causes some clogging in the orifice nozzle, the droplets' acceleration will be changed. Droplet distortion would force droplets into an oblate spheroid which means a higher drag than a spherical shape (of same volume). This would increase the acceleration to give a higher droplet velocity in the measurement zone of APS, which leads to error in aerodynamic droplet sizing. Higher velocity would mean a smaller droplet aerodynamic size.

It has been found in literature that the evaporated model saliva droplets (composed of NaCl-mucin mixture or NaCl-protein mixture) may evolve into semi-solid and semi-liquid phase state in the evaporation process (Huynh et al. 2022). The high contents of mucin in the saliva droplets would cause the moisture release process to be delayed and the droplets become viscous on drying which might impede the water evaporation (Walker et al. 2021). The artificial saliva droplet in our experiment could be evaporated into a semi-solid phase, and its shape might be distorted when going through the orifice nozzle of APS, leading to droplet over-speeding and undersizing by APS. Compared with the saline droplet (which is in solid phase after evaporation), this would mean that the artificial saliva droplet sizing could incur droplet distortion and larger deviations from the reference VED value. High-viscosity of artificial saliva droplets could also cause sizing errors when measured by APS (Bartley et al. 2000).

5.2 Uncertainty in droplet effective density

The conventional practice is to use PSL particles with certified diameter as traceable reference size standard for particle sizer calibration. It has been shown that the deviation of effective particle density from that of PSL particle could affect APS sizing with oversizing errors (Ananth and Wilson 1988; Wang and John 1987; Baron 1986). Therefore, we have applied density correction to the aerodynamic diameter indicated by APS, based on the estimated effective

density for saline and saliva droplets and the theoretical correction factors given in (Ananth and Wilson 1988).

However, there is some uncertainty in the effective density estimation and DSF for the saline or saliva droplets. Thus, there would be some uncertainty in the density correction factors applied to the aerodynamic diameter reading by APS. Hence some errors in the reference VED for saline and saliva droplets can be expected.

5.3 Spray generator effect

There is a flowrate control knob in the ULV droplet generator. Although all four metrology institutes have used the same setting for this flowrate knob, there is some uncertainty in the actual liquid flowrate in the spray generator. Variation in liquid flowrate could cause changes in the polydisperse droplets' size distribution. Therefore, this effect might lead to some variation on the droplets' TVC-size distribution.

The reported VED of droplets was based on the peak position of the droplets' TVC-size distribution, thus the repeatability of ULV spray generator could lead to some error in the reported VED of droplets measured by each laboratory.

5.4 Conversion of aerodynamic diameter

The conversion from aerodynamic diameter to optical equivalent diameter using (3) requires accurate values for DSF and droplet material density. However, there are uncertainties in the value of DSF for NaCl particles (Zelenyuk et al. 2006; Slowik et al. 2004; Marshall et al. 1991; Brockmann and Rader 1990; Cartwright 1962). The bounds of DSF values for NaCl particles near 4 μm can be assumed to be [1.14, 1.40], based on (Zelenyuk et al. 2006). The potential relative error in the estimated material density of dried saliva droplet is up to 5.3%. Thus, the random error in DSF and material density would lead to some potential errors in saline and saliva droplets' VED (measured by APS), which is due to the conversion from aerodynamic diameter to optical equivalent diameter.

5.5 Particle shape and refractive index

The saline droplets have non-spherical shape (cubic shape) which can generate higher light-scattering compared to that predicted by Mie scattering theory for particles with spherical shape (Curtis et al. 2008; Chamaillard et al. 2003; Friehmelt and Heidenreich 1999; Gebhart 1991; Buettner 1990; Büttner 1983). The OPSS sizing was calibrated by certified spherical PSL particles which produced light scattering with close matching to the theoretic Mie scattering values. Therefore, we have seen oversizing error up to 14.8% for the saline droplets measured by OPSS, which is due to their non-spherical shape and increased light-scattering.

The refractive index (real part) of saline and saliva droplets are different from that of PSL particles (Kasarova et al. 2007; Nikolov and Ivanov 2000; McMeekin et al. 1962, 1964). Thus the light scattering from these droplets would have deviations compared to the PSL particles (Rosenberg et al. 2012; Liu and Daum 2000). Therefore, the OPSS would give some sizing error for the saline and saliva droplets, due to the deviations in the refractive index.

5.6 Lack of reference size standard and traceability

There is a lack of traceability for saline or saliva droplet size measurement since PSL particle is unsuitable as traceable reference size standard for saliva and saline droplets. The DSF and refractive index of saline droplet is also different from that of PSL particle. To the best of our knowledge, no national metrology institute (NMI) has established droplet size metrology standard for saline or artificial saliva droplet with proper traceability.

To address the issues in saliva and saline droplet size measurement, NMIs need to develop reference droplet generator which can produce mono-dispersed saliva & saline droplets. Further study is needed on the DSF of such reference droplets. The effect of irregular shape and refractive index variation for droplet sizing using OPSS need to be studied. Such supermicron reference size standards (1-20 μm) for saliva and saline droplet measurement would help to improve the measurement accuracy and establish traceability in saliva & saline droplet size measurement.

6. Conclusion

An evaluation of the saline and artificial saliva droplet size measurement accuracy has been reported in this paper. We have selected to use artificial saliva and saline solutions of 18.1% (w/w) and 6.5% (w/w) to produce polydisperse droplets by a ULV spray generator. A special test chamber was designed for droplet sampling and measurement. In this inter-laboratory comparison study, we have defined the measurand as the VED size corresponding to the peak in the droplets' TVC-size distribution. The traveling standard (droplet generator coupled with test chamber) had been circulated among four metrology institutes (NMC, CMS/ITRI, NIM, KRISS) to make droplet size measurement by particle sizers (OPSS or APS). The composition of artificial saliva had been analysed with good accuracy, which is used to estimate the material density of dried artificial saliva droplet.

The comparison between four institutes have shown that, for saliva droplets, the VED size deviations from the reference VED values (around 4 μm) are below 5.3% for OPSS measurement. For saliva droplet sizes measured by APS, one institute showed deviation below 7.6% and two institutes showed higher deviations up to 21.9% from the reference VED values. For saline droplet size measurement, the deviations from the reference VED values were below 10.0% for APS measurement. The saline droplet size measured by OPSS exceeds the reference VED with a

relative deviation of up to 14.8%, which is due to the increased light scattering from the non-spherical NaCl particles. Various potential errors in droplet size measurement have been discussed.

We have investigated the saline and artificial saliva droplet size measurement accuracy (by OPSS and APS) with well-designed traveling standard and experimental setup, for the first time among all NMIs. It is found that new reference size standards for artificial saliva and saline droplet measurement would be needed to improve the accuracy. More research work would be needed to establish traceability for measurement of saline or saliva droplets' size. Such reference standards can support the calibration of commercial particle sizers. The artificial saliva droplets can be used to simulate human speech or cough droplets for evaluation of size measurement accuracy. More accurate saliva droplet size measurement will enable reliable characterization of human speech and cough droplet size distribution in future for effective infection control.

Acknowledgements This study is supported by the APMP's Response Programme against COVID-19 under Project: COVID-2020-01. The authors would like to thank Dr. Andrea Tiwari and Dr. Torsten Tritscher for the helpful discussion on droplet size measurement using aerodynamic particle sizer.

Compliance with ethical standards

Conflict of interest On behalf of all authors, the corresponding author states that there is no conflict of interest.

Reference

Ananth, G. and Wilson, J.C. (1988). Theoretical analysis of the performance of the tsi aerodynamic particle sizer: The effect of density on response. *Aerosol Sci. Technol.* 9 (3):189–199. doi:10.1080/02786828808959207.

Asadi, S., Bouvier, N., Wexler, A.S., and Ristenpart, W.D. (2020). The coronavirus pandemic and aerosols: Does COVID-19 transmit via expiratory particles? *Aerosol Sci. Technol.*

ASTM (2016a). ASTM E2721-16, Standard Practice for Evaluation of Effectiveness of Decontamination Procedures for Surfaces When Challenged with Droplets Containing Human Pathogenic Viruses.

ASTM (2016b). ASTM E2720-16, Standard Practice for Evaluation of Effectiveness of Decontamination Procedures for Air-Permeable Materials when Challenged with Biological Aerosols Containing Human Pathogenic Viruses.

Azodo, C.C. and Osahon, O.D. (2020). Quantitative and Qualitative Analysis of Relative Saliva Viscosity among Carious and Non-Carious Young Adults. *Niger. J. Dent. Res.* 5 (2):131–135.

Baron, P., Deye, G.J., Martinez, A.B., Jones, E.N., and Bennett, J.S. (2008). Size Shifts in Measurements of Droplets with the Aerodynamic Particle Sizer and the Aerosizer. *Aerosol Sci. Technol.* 42 (3):201–209. doi:10.1080/02786820801958734.

Baron, P.A. (1986). Calibration and use of the aerodynamic particle sizer (APS 3300). *Aerosol Sci. Technol.* 5 (1):55–67. doi:10.1080/02786828608959076.

Bartley, D.L., Martinez, A.B., Baron, P.A., Secker, D.R., and Hirst, E. (2000). Droplet distortion in accelerating flow. *J. Aerosol Sci.* 31 (12):1447–1460. doi:10.1016/S0021-8502(00)00042-2.

Bemer, D., Fabries, J.F., and Renoux, A. (1990). Calculation of the theoretical response of an optical particle counter and its practical usefulness. *J. Aerosol Sci.* 21 (5):689–700.

Bourouiba, L. (2021). Fluid Dynamics of Respiratory Infectious Diseases. *Annu. Rev. Biomed. Eng.* 23:547–577. doi:10.1146/ANNUREV-BIOENG-111820-025044.

Bourouiba, L. (2020). Transport of Droplets and Aerosols in Respiratory Activities*., in US Nat. Academies of Sci., Engr., and Med. - Airborne Transmission of SARS-CoV-2: A Virtual Workshop, .*

Bourouiba, L., Dehandschoewercker, E., and Bush, J.W.M. (2014). Violent expiratory events: On coughing and sneezing. *J. Fluid Mech.* 745:537–563. doi:10.1017/JFM.2014.88.

Brockmann, J.E. and Rader, D.J. (1990). Aps response to nonspherical particles and experimental determination of dynamic shape factor. *Aerosol Sci. Technol.* 13 (2):162–172. doi:10.1080/02786829008959434.

Buettner, H. (1990). Measurement of the size of fine nonspherical particles with a light-scattering particle counter. *Aerosol Sci. Technol.* 12 (2):413–421. doi:10.1080/02786829008959356.

Büttner, H. (1983). Kalibrierung einer Streulicht-Meßeinrichtung zur Partikelgrößenanalyse mit Impaktoren. *Chemie Ing. Tech.* 55 (1):65. doi:10.1002/cite.330550123.

Cartwright, J. (1962). Particle Shape Factors. *Ann. Occup. Hyg.* 5 (3):163–171.

Chamaillard, K., Jennings, S.G., Kleefeld, C., Ceburnis, D., and Yoon, Y.J. (2003). Light backscattering and scattering by nonspherical sea-salt aerosols. *J. Quant. Spectrosc. Radiat. Transf.* 79–80:577–597. doi:10.1016/S0022-4073(02)00309-6.

Chao, C.Y.H., Wan, M.P., Morawska, L., Johnson, G.R., Ristovski, Z.D., Hargreaves, M., Mengersen, K., Corbett, S., Li, Y., Xie, X., and Katoshevski, D. (2009). Characterization of expiration air jets and droplet size distributions immediately at the mouth opening. *J. Aerosol Sci.* 40 (2):122–133.

Chaudhuri, S., Basu, S., Kabi, P., Unni, V.R., and Saha, A. (2020). Modeling the role of respiratory droplets in Covid-19 type pandemics. *Phys. Fluids* 32 (6).

Chen, B.T., Cheng, Y.S., and Yeh, H.C. (1985). Performance of a TSI aerodynamic particle sizer. *Aerosol Sci. Technol.* 4 (1):89–97. doi:10.1080/02786828508959041.

Chen, B.T., Cheng, Y.S., and Yeh, H.C. (1984). Experimental responses of two optical particle counters. *J. Aerosol Sci.* 15 (4):457–464.

Chien, C.H., Theodore, A., Wu, C.Y., Hsu, Y.M., and Birky, B. (2016). Upon correlating diameters measured by optical particle counters and aerodynamic particle sizers. *J. Aerosol Sci.* 101:77–85. doi:10.1016/j.jaerosci.2016.05.011.

Curtis, D.B., Meland, B., Aycibin, M., Arnold, N.P., Grassian, V.H., Young, M.A., and Kleiber, P.D. (2008). A laboratory investigation of light scattering from representative components of mineral dust aerosol at a wavelength of 550 nm. *J. Geophys. Res. Atmos.* 113 (D8):8210. doi:10.1029/2007JD009387.

Czitrovszky, A. (2010). Applications of Optical Methods for Micrometer and Submicrometer Particle Measurements*., in Aerosols - Science and Technology,* Wiley-VCH, pp. 203–239.

De Oliveira, P.M., Mesquita, L.C.C., Gkantonas, S., Giusti, A., and Mastorakos, E. (2021). Evolution of spray and aerosol from respiratory releases: theoretical estimates for insight on viral transmission. *Proc. R. Soc. A* 477 (2245). doi:10.1098/RSPA.2020.0584.

DeCarlo, P.F., Slowik, J.G., Worsnop, D.R., Davidovits, P., and Jimenez, J.L. (2004). Particle morphology and density characterization by combined mobility and aerodynamic diameter measurements. Part 1: Theory. *Aerosol Sci. Technol.* 38 (12):1185–1205. doi:10.1080/027868290903907.

Duguid, J.P. (1946). The size and the duration of air-carriage of respiratory droplets and droplet-nuclei. *J. Hyg. (Lond).* 44 (6):471–479. doi:10.1017/S0022172400019288.

Eraga, S.O., Ofeogbu, P.U., Ovu, E.O., and Iarhewoh, M. (2016). An investigation of the properties of mucin obtained from three sources. *Pharma Innov. J.* 5 (12):8–12.

Fennelly, K.P. (2020). Particle sizes of infectious aerosols: implications for infection control. *Lancet Respir. Med.* 8 (9):914–924.

Friehmelt, R. and Heidenreich, S. (1999). Calibration of a white-light/90° optical particle counter for "aerodynamic" size measurements experiments and calculations for spherical particles and quartz dust. *J. Aerosol Sci.* 30 (10):1271–1279. doi:10.1016/S0021-8502(99)00044-0.

Gebhart, J. (1991). Response of Single-Particle Optical Counters to Particles of irregular shape. *Part. Part. Syst. Charact.* 8 (1–4):40–47. doi:10.1002/PPSC.19910080109.

Gralton, J., Tovey, E., McLaws, M.L., and Rawlinson, W.D. (2011). The role of particle size in aerosolised pathogen transmission: A review. *J. Infect.* 62 (1):1–13. doi:10.1016/J.JINF.2010.11.010.

Griffiths, W.D., Patrick, S., and Rood, A.P. (1984). An aerodynamic particle size analyser tested with spheres, compact particles and fibres having a common settling rate under gravity. *J. Aerosol Sci.* 15 (4):491–502. doi:10.1016/0021-8502(84)90045-4.

Hand, J.L. and Kreidenweis, S.M. (2002). A new method for retrieving particle refractive index and effective density from aerosol size distribution data. *Aerosol Sci. Technol.* 36 (10):1012–1026. doi:10.1080/02786820290092276.

Hasan, H. and Dzubay, T.G. (1983). Apportioning light extinction coefficients to chemical species in atmospheric aerosol. *Atmos. Environ.* 17 (8):1573–1581. doi:10.1016/0004-6981(83)90310-4.

Haynes, W.M. (2016). CRC Handbook of Chemistry and Physics*, CRC Handbook of Chemistry and Physics*. CRC Press.

Heidenreich, S., Büttner, H., and Ebert, F. (1995). Investigations on the Behaviour of an Aerodynamic Particle Sizer and its applicability to calibrate an optical particle counter. *Part. Part. Syst. Charact.* 12 (6):304–308. doi:10.1002/ppsc.19950120610.

Huynh, E., Olinger, A., Woolley, D., Kohli, R.K., Choczynski, J.M., Davies, J.F., Lin, K., Marr, L.C., and Davis, R.D. (2022). Evidence for a semisolid phase state of aerosols and droplets relevant to the airborne and surface survival of pathogens. *Proc. Natl. Acad. Sci. U. S. A.* 119 (4):e2109750119. doi:10.1073/pnas.2109750119.

Iida, K. and Sakurai, H. (2018). Counting efficiency evaluation of optical particle counters in micrometer range by using an inkjet aerosol generator. *Aerosol Sci. Technol.* 1156–1166.

Iida, K., Sakurai, H., Saito, K., and Ehara, K. (2014). Inkjet aerosol generator as monodisperse particle number standard. *Aerosol Sci. Technol.* 48 (8):789–802.

ISO (2018). ISO 21501-4:2018 - Determination of particle size distribution — Single particle light interaction methods — Part 4: Light scattering airborne particle counter for clean spaces.

ISO (2009). ISO 21501-1:2009 - Determination of particle size distribution — Single particle light interaction methods — Part 1: Light scattering aerosol spectrometer.

ISO (2008). ISO/IEC Guide 98-3:2008 - Uncertainty of measurement — Part 3: Guide to the expression of uncertainty in measurement (GUM:1995).

Johnston, H.L. and Hutchison, D.A. (1942). Density of Sodium Chloride The Atomic Weight of Fluorine by Combination of Crystal Density and X-Ray Data. *Phys. Rev.* 62 (1–2):32.

Kasarova, S.N., Sultanova, N.G., Ivanov, C.D., and Nikolov, I.D. (2007). Analysis of the dispersion of optical plastic materials. *Opt. Mater. (Amst).* 29 (11):1481–1490.

Kramm, K., Orth, M., Teiwes, A., Kammerhofer, J.C., Meunier, V., Pietsch-Braune, S., and Heinrich, S. (2023). Influence of Nozzle Parameters on Spray Pattern and Droplet Characteristics for a Two-Fluid Nozzle. *Chemie Ing. Tech.* 95 (1–2):151–159. doi:10.1002/cite.202200152.

Kuwata, M. and Kondo, Y. (2009). Measurements of particle masses of inorganic salt particles for calibration of cloud condensation nuclei counters. *Atmos. Chem. Phys.* 9 (16):5921–5932. doi:10.5194/acp-9-5921-2009.

Langmuir, A.D. (1951). The potentialities of biological warfare against man. An epidemiological appraisal. *Public Heal. reports (Washington, D.C. 1896)* 66 (13):387–399. doi:10.2307/4587679.

Liu, H.; Xu, B.; Cao, W-L.; Dai, X.-H. (2010). Determination of urea in human serum using isotope-dilution liquid chromatography/tandem mass spectrometry. *Chin. J. Anal. Lab.* (6):27–30.

Liu, B.Y.H., Szymanski, W.W., and Ahn, K.H. (1985). On aerosol size distribution measurement by laser and white light optical particle counters. *J. Environ. Sci.* 28 (3):19–24. doi:10.17764/jiet.1.28.3.k873425806586048.

Liu, Y. and Daum, P.H. (2000). The effect of refractive index on size distributions and light scattering coefficients derived from optical particle counters. *J. Aerosol Sci.* 31 (8):945–957. doi:10.1016/S0021-8502(99)00573-X.

Mäkynen, J., Hakulinen, J., Kivistö, T., and Lehtimäki, M. (1982). Optical particle counters: Response, resolution and counting efficiency. *J. Aerosol Sci.* 13 (6):529–535. doi:10.1016/0021-8502(82)90018-0.

Mari, L. (2015). Evolution of 30 years of the International Vocabulary of Metrology (VIM). *Metrologia* 52 (1):R1–R10. doi:10.1088/0026-1394/52/1/R1.

Marshall, I.A., Mitchell, J.P., and Griffiths, W.D. (1991). The behaviour of regular-shaped non-spherical particles in a TSI aerodynamic particle sizer. *J. Aerosol Sci.* 22 (1):73–89. doi:10.1016/0021-8502(91)90094-X.

McMeekin, T.L., Groves, M.L., and Hipp, N.J. (1964). Refractive Indices of Amino Acids, Proteins, and Related Substances*., in ADVANCES IN CHEMISTRY SERIES,* pp. 54–66.

McMeekin, T.L., Wilensky, M., and Groves, M.L. (1962). Refractive indices of proteins in relation to amino acid composition and specific volume. *Biochem. Biophys. Res. Commun.* 7 (2):151–156. doi:10.1016/0006-291X(62)90165-1.

Morawska, L. and Cao, J. (2020). Airborne transmission of SARS-CoV-2: The world should face the reality. *Environ. Int.* 139:105730.

Morawska, L., Johnson, G.R., Ristovski, Z.D., Hargreaves, M., Mengersen, K., Corbett, S., Chao, C.Y.H., Li, Y., and Katoshevski, D. (2009). Size distribution and sites of origin of droplets expelled from the human respiratory tract during expiratory activities. *J. Aerosol Sci.* 40 (3):256–269.

NASEM (2020). Airborne Transmission of SARS-CoV-2: Proceedings of a Workshop—in Brief, National Academies of Science, Engineering and Medicine*, Airborne Transmission of SARS-CoV-2*. National Academies Press.

Nasr, G.G., Yule, A.J., and Bendig, L. (2002). Industrial Sprays and Atomization*, Industrial Sprays and Atomization*. Springer London.

Netz, R.R. (2020). Mechanisms of Airborne Infection via Evaporating and Sedimenting Droplets Produced by Speaking. *J. Phys. Chem. B* 124 (33):7093–7101. doi:10.1021/ACS.JPCB.0C05229.

Netz, R.R. and Eaton, W.A. (2020). Physics of virus transmission by speaking droplets. *Proc. Natl. Acad. Sci. U. S. A.* 117 (41):25209–25211. doi:10.1073/pnas.2011889117.

Nguyen, D.A. and Rhodes, M.J. (1998). Producing fine drops of water by twin-fluid atomisation. *Powder Technol.* 99 (3):285–292. doi:10.1016/S0032-5910(98)00125-9.

Nicas, M., Nazaroff, W.W., and Hubbard, A. (2005). Toward understanding the risk of secondary airborne infection: Emission of respirable pathogens. *J. Occup. Environ. Hyg.* 2 (3):143–154. doi:10.1080/15459620590918466.

Nikolov, I.D. and Ivanov, C.D. (2000). Optical plastic refractive measurements in the visible and the near-infrared regions. *Appl. Opt.* 39 (13):2067. doi:10.1364/AO.39.002067.

Papineni, R.S. and Rosenthal, F.S. (1997). The size distribution of droplets in the exhaled breath of healthy human subjects. *J. Aerosol Med.* 10 (2):105–116.

Pavese, F. (2007). The definition of the measurand in key comparisons: Lessons learnt with thermal standards. *Metrologia* 44 (5):327–339. doi:10.1088/0026-1394/44/5/009.

Peters, T.M., Ott, D., and O'Shaughnessy, P.T. (2006). Comparison of the Grimm 1.108 and 1.109 Portable Aerosol Spectrometer to the TSI 3321 Aerodynamic Particle Sizer for Dry Particles. *Ann. Occup. Hyg.* 50 (8):843–850. doi:10.1093/annhyg/mel067.

Randall, K., Ewing, E.T., Marr, L.C., Jimenez, J.L., and Bourouiba, L. (2021). How did we get here: what are droplets and aerosols and how far do they go? A historical perspective on the transmission of respiratory infectious diseases. *Interface Focus* 11 (6). doi:10.1098/RSFS.2021.0049.

Redrow, J., Mao, S., Celik, I., Posada, J.A., and gang Feng, Z. (2011). Modeling the evaporation and dispersion of airborne sputum droplets expelled from a human cough. *Build. Environ.* 46 (10):2042–2051. doi:10.1016/J.BUILDENV.2011.04.011.

Rezaei, M. and Netz, R.R. (2021). Airborne virus transmission via respiratory droplets: Effects of droplet evaporation and sedimentation. *Curr. Opin. Colloid Interface Sci.* 55:101471. doi:10.1016/J.COCIS.2021.101471.

Rosenberg, P.D., Dean, A.R., Williams, P.I., Dorsey, J.R., Minikin, A., Pickering, M.A., and Petzold, A. (2012). Particle sizing calibration with refractive index correction for light scattering optical particle counters and impacts upon PCASP and CDP data collected during the Fennec campaign. *Atmos. Meas. Tech.* 5 (5):1147–1163. doi:10.5194/amt-5-1147-2012.

Sang-Nourpour, N. and Olfert, J.S. (2019). Calibration of optical particle counters with an aerodynamic

aerosol classifier. *J. Aerosol Sci.* 138:105452.

Sargent, M., Harte, R., and Harrington, C. (2002). Guidelines for Achieving High Accuracy in Isotope Dilution Mass Spectrometry (IDMS). Royal Society of Chemistry.

Slowik, J.G., Stainken, K., Davidovits, P., Williams, L.R., Jayne, J.T., Kolb, C.E., Worsnop, D.R., Rudich, Y., DeCarlo, P.F., and Jimenez, J.L. (2004). Particle morphology and density characterization by combined mobility and aerodynamic diameter measurements. Part 2: Application to combustion-generated soot aerosols as a function of fuel equivalence ratio. *Aerosol Sci. Technol.* 38 (12):1206–1222. doi:10.1080/027868290903916.

Stadnytskyi, V., Bax, C.E., Bax, A., and Anfinrud, P. (2020). The airborne lifetime of small speech droplets and their potential importance in SARS-CoV-2 transmission. *Proc. Natl. Acad. Sci. U. S. A.* 117 (22):11875–11877. doi:10.1073/pnas.2006874117.

Szymanski, W.W. and Liu, B.Y.H.H. (1986). On the Sizing Accuracy of Laser Optical Particle Counters. *Part. Part. Syst. Charact.* 3 (1):1–7. doi:10.1002/PPSC.19860030102.

Szymanski, W.W., Nagy, A., and Czitrovszky, A. (2009). Optical particle spectrometry-Problems and prospects. *J. Quant. Spectrosc. Radiat. Transf.* 110 (11):918–929.

van der Meulen, A., Plomp, A., Oeseburg, F., Buringh, E., van Aalst, R.M., and Hoevers, W. (1980). Intercomparison of optical particle counters under conditions of normal operation. *Atmos. Environ.* 14 (4):495–499.

Vasilatou, K., Dirscherl, K., Iida, K., Sakurai, H., Horender, S., and Auderset, K. (2020). Calibration of optical particle counters: First comprehensive inter-comparison for particle sizes up to 5 μm and number concentrations up to 2 cm-3. *Metrologia* 25005.

Vasilatou, K., Wälchli, C., Koust, S., Horender, S., Iida, K., Sakurai, H., Schneider, F., Spielvogel, J., Wu, T.Y., and Auderset, K. (2021). Calibration of optical particle size spectrometers against a primary standard: Counting efficiency profile of the TSI Model 3330 OPS and Grimm 11-D monitor in the particle size range from 300 nm to 10 μm. *J. Aerosol Sci.* 157:105818.

Walker, J.S., Archer, J., Gregson, F.K.A., Michel, S.E.S., Bzdek, B.R., and Reid, J.P. (2021). Accurate Representations of the Microphysical Processes Occurring during the Transport of Exhaled Aerosols and Droplets. *ACS Cent. Sci.* 7 (1):200–209. doi:10.1021/acscentsci.0c01522.

Wang, C.C., Prather, K.A., Sznitman, J., Jimenez, J.L., Lakdawala, S.S., Tufekci, Z., and Marr, L.C. (2021). Airborne transmission of respiratory viruses. *Science (80-.).* 373 (6558). doi:10.1126/SCIENCE.ABD9149.

Wang, H.-C.C. and John, W. (1987). Particle Density Correction for the Aerodynamic Particle Sizer. *Aerosol Sci. Technol.* 6 (2):191–198. doi:10.1080/02786828708959132.

Wang, X., Chancellor, G., Evenstad, J., Farnsworth, J.E., Hase, A., Olson, G.M., Sreenath, A., and Agarwal, J.K. (2009). A novel optical instrument for estimating size segregated aerosol mass concentration in real time. *Aerosol Sci. Technol.* 43 (9):939–950. doi:10.1080/02786820903045141.

Wells, W.F. (1934). On air-borne infection: Study II. Droplets and droplet nuclei. *Am. J. Epidemiol.* 20 (3):611–618. doi:10.1093/OXFORDJOURNALS.AJE.A118097.

WHO (2020). The International Pharmacopoeia, 10th ed.

Wu, T.Y. (2022). Investigation of artificial saliva and saline droplet size measurement for COVID-19 infection control*., in APMP Webinar on APMP's Responses to COVID-19,* .

Wu, T.Y., Horender, S., Tancev, G., and Vasilatou, K. (2022a). Evaluation of aerosol-spectrometer based PM2.5 and PM10 mass concentration measurement using ambient-like model aerosols in the laboratory. *Measurement* 201:111761. doi:10.1016/j.measurement.2022.111761.

Wu, T.Y., Murashima, Y., Sakurai, H., and Iida, K. (2022b). A bilateral comparison of particle number concentration standards via calibration of an optical particle counter for number concentration up to ~1000 cm−3. *Measurement* 189:110446. doi:10.1016/j.measurement.2021.110446.

Xie, X., Li, Y., Chwang, A.T.Y., Ho, P.L., and Seto, W.H. (2007). How far droplets can move in indoor environments - revisiting the Wells evaporation-falling curve. *Indoor Air* 17 (3):211–225.

Xu, C., Ding, Y., Leung, H.W., Tong, B.M.K., Shin, R.Y.C., and Lee, T.K. (2017). Development of high accuracy methods for the certification of calcium, iron, magnesium and potassium in human serum. *J. Trace Elem. Med. Biol.* 40:61–66.

Yang, S., Lee, G.W.M., Chen, C.M., Wu, C.C., and Yu, K.P. (2007). The size and concentration of droplets generated by coughing in human subjects. *J. Aerosol Med.* 20 (4):484–494. doi:10.1089/jam.2007.0610.

Yli-Ojanperä, J., Sakurai, H., Iida, K., Mkel, J.M., Ehara, K., and Keskinen, J. (2012). Comparison of three particle number concentration calibration standards through calibration of a single CPC in a wide particle size range. *Aerosol Sci. Technol.* 1163–1173.

Yu, W.Z., Liu, Q., Leung, H.W., Tong, B.M.K., Chew, G., Lee, T.K., Shin, R.Y.C., Teo, T.L., and Sethi, S.K. (2021). Improving the accuracy of chloride measurements through participation in regular external quality assessment programme. *J. Trace Elem. Med. Biol.* 68:126825.

Zelenyuk, A., Cai, Y., and Imre, D. (2006). From Agglomerates of Spheres to Irregularly Shaped Particles: Determination of Dynamic Shape Factors from Measurements of Mobility and Vacuum Aerodynamic Diameters. *Aerosol Sci. Technol.* 40 (3):197–217.